



UNIVERSITY OF LEEDS

This is a repository copy of *Using the National Radiotherapy Dataset within the National Cancer Data Repository to investigate patterns of use of radiotherapy in the management of surgically treated rectal cancer across the English NHS*.

White Rose Research Online URL for this paper:  
<http://eprints.whiterose.ac.uk/87840/>

Version: Accepted Version

---

**Article:**

Morris, E, Finan, P, Thomas, J et al. (4 more authors) (2015) Using the National Radiotherapy Dataset within the National Cancer Data Repository to investigate patterns of use of radiotherapy in the management of surgically treated rectal cancer across the English NHS. *European Journal of Cancer Care*, 24 (S1). 20 - 21. ISSN 0961-5423

---

**Reuse**

Unless indicated otherwise, fulltext items are protected by copyright with all rights reserved. The copyright exception in section 29 of the Copyright, Designs and Patents Act 1988 allows the making of a single copy solely for the purpose of non-commercial research or private study within the limits of fair dealing. The publisher or other rights-holder may allow further reproduction and re-use of this version - refer to the White Rose Research Online record for this item. Where records identify the publisher as the copyright holder, users can verify any specific terms of use on the publisher's website.

**Takedown**

If you consider content in White Rose Research Online to be in breach of UK law, please notify us by emailing [eprints@whiterose.ac.uk](mailto:eprints@whiterose.ac.uk) including the URL of the record and the reason for the withdrawal request.



[eprints@whiterose.ac.uk](mailto:eprints@whiterose.ac.uk)  
<https://eprints.whiterose.ac.uk/>

**An infinite chainmail of  $M_6L_6$  metallacycles featuring multiple  
Borromean links**

Flora L. Thorp-Greenwood, Alexander N. Kulak and Michael J. Hardie\*

School of Chemistry, University of Leeds, Woodhouse Lane, Leeds, LS2 9JT, UK

\*To whom correspondence should be addressed. Email: [m.j.hardie@leeds.ac.uk](mailto:m.j.hardie@leeds.ac.uk)

## Abstract

Borromean rings or links are topologically complex assemblies of three entangled rings where no two rings are interlinked in a chain-like catenane, yet the three rings cannot be separated. We report here a metallacycle complex whose crystalline network forms the first example of a new class of entanglement. The complex is formed from the self-assembly of  $\text{CuBr}_2$  with the cyclotrimeratrylene-scaffold ligand  $(\pm)$ -tris(iso-nicotinoyl)cyclotriguaiacylene. Individual metallacycles are interwoven into a 2D chainmail network where each metallacycle exhibits multiple Borromean ring-like associations with its neighbours. This only occurs in the solid state, and also represents the first example of a crystalline infinite chainmail 2D network. Crystals of the complex were twinned and have an unusual hollow tubular morphology likely resulting from a localised dissolution-recrystallisation process.

## Main Text

The ability of chemical systems to form topologically complicated threaded architectures has long fascinated chemists.<sup>1</sup> These involve either a single molecular component which is self-entangled such as in a knot; or feature two or more components that are mechanically linked together but are chemically independent, that is, the components are not connected through covalent or dative bonds. The best known threaded architectures are catenanes, rotaxanes and knots.<sup>1-3</sup> Catenanes have chemically-independent macrocyclic components connected through a mechanical chain-link arrangement, shown schematically in Fig. 1a, while rotaxanes feature a rod-through-macrocycle arrangement.<sup>1</sup> Catenane and rotaxane systems may have applications as molecular machines<sup>4,5</sup> including within electronic devices,<sup>6</sup> and in synthesis.<sup>7</sup> As well as knots, simple catenanes and rotaxanes, known complex chemical topologies include: cage catenanes and multicatenanes,<sup>8-12</sup> Star of David catenane,<sup>13</sup> Solomon's links,<sup>14</sup> Borromean rings<sup>15-19</sup> and a molecular ravel.<sup>20</sup> Topologically complex structural relationships can also be found in network materials such as coordination polymers. Coordination polymers are crystalline assemblies of metal cations and bridging organic ligands with infinite 2D or 3D network structures. Whole coordination networks may be entangled through interpenetration or polycatenation,<sup>21-23</sup> and infinite networks have been reported to form through catenane formation between chemically independent rings<sup>24,25</sup> catenane formation between 1D coordination polymers,<sup>26</sup> or between 3D metallo-cages.<sup>27,28</sup>

A Borromean ring or link is composed of three independent rings that are linked together but where no two rings are interlocked into a catenane. They have three principal representations: orthogonal rings, chain rings and Venn rings (Fig. 1b). Borromean rings are an example of a

Brunnian link, meaning that if any one ring is cut then the assembly can be completely separated. Examples of discrete chemical Borromean ring systems are rare. Seeman and co-workers have constructed Borromean rings from DNA.<sup>15</sup> Stoddart used an elegant strategy based on metal-directed self-assembly with concurrent labile organic bond formation with subsequent demetallation giving the independent rings.<sup>16,17</sup> Jin and co-workers have recently reported a short series of Borromean ring assemblies formed by rectangular metallacycles.<sup>18,19</sup> Metallated Borromean assemblies where three macrocyclic ligands have a Borromean association but are held together through endo and exo metal-ligand coordination are also known<sup>17,29,30</sup> and may be a precursor to “real” Borromean rings.<sup>16</sup> Conceptually similar but topologically non-complex ring-in-ring assemblies with two macrocycles have been reported as steps towards Borromean rings.<sup>31</sup>

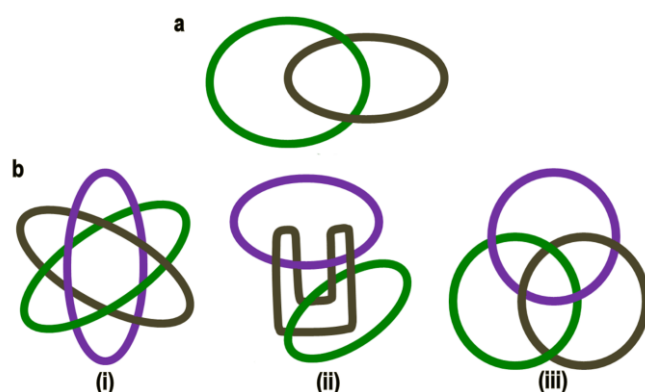
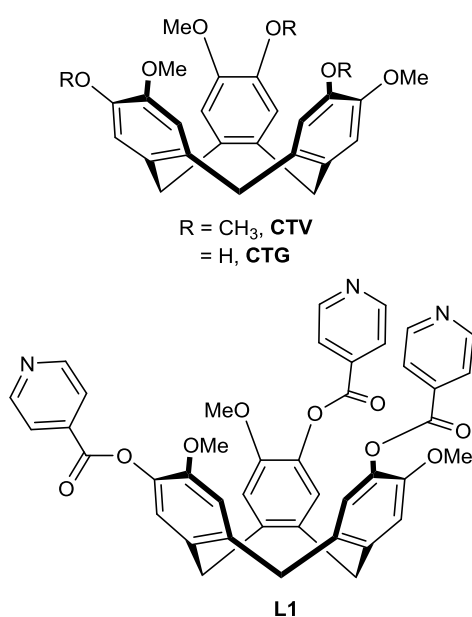


**Figure 1. Examples of entangled ring assemblies.** (a) [2]catenane which forms a chain-like linkage between individual rings; (b) three representations of Borromean rings which do not feature a chain-like link yet cannot be separated without breakage: (i) orthogonal rings, (ii) chain rings, (iii) Venn rings.

The formation of Borromean entanglements within crystalline network materials such as coordination polymers was first recognized by Ciani and co-workers,<sup>32</sup> and is often referred to as a Borromean weave. Since then, a number of 2D coordination polymers that exhibit a Borromean weave have been reported, and examples have been compiled within two articles.<sup>21,33</sup> In all the cases that we are aware of, the Borromean structural relationships in a Borromean weave are between infinite connected networks. We report herein the first example of a network that is formed by entangled but independent discrete rings to form a 2D chainmail motif which contains multiple Borromean-like associations. This occurs from the self-assembly of  $\text{CuBr}_2$  and a cavitand ligand with a cyclotrimeratrylene (CTV) scaffold,  $(\pm)$ -tris(iso-nicotinoyl)cyclotriguaiacylene **L1**. Interestingly, this is also the first example of a crystalline infinite 2D chainmail motif regardless of the manner of entanglement.

**CTV** and its chiral analogue cyclotriguaiacylene (**CTG**) are molecular hosts capable of binding guest molecules within a bowl-shaped molecular cavity, hence may be referred to as cavitand molecules. Cavitand molecules based on a **CTV**-scaffold have been utilized in a number of applications in supramolecular chemistry and soft materials.<sup>34</sup> This includes their use as components of coordination polymers and of discrete metallo-supramolecular cage-like assemblies, including the topologically complex assemblies of triply interlocking cage-catenane species<sup>10,11</sup> and a self-entangled Solomon's cube.<sup>35</sup> The cavitand ( $\pm$ )-tris(iso-nicotinoyl)cyclotriguaiacylene, **L1**, has been previously reported<sup>36</sup> and forms metallo-cage species with Pd(II), namely an octahedral  $[\text{Pd}_6(\mathbf{L1})_8]^{12+}$  stella octangula cage<sup>37</sup> and a  $[\text{Pd}_3(\text{bis-NHC})_3(\mathbf{L1})_2]^{6+}$  metallo-capsule where bis-NHC is a chelating bis-carbene ligand.<sup>48</sup> Ligand **L1** also forms a 2D coordination polymer with Ag(I).<sup>36</sup>



## Results and Discussion

Addition of ligand ( $\pm$ )-**L1** dissolved in  $\text{CH}_3\text{NO}_2$  to a solution of 2 equivalents of  $\text{CuBr}_2$  in dimethylsulfoxide (DMSO) resulted in growth of yellow-green crystals of complex **1** with overall composition  $[\text{Cu}_6\text{Br}_{10}(\text{DMSO})_6(\text{H}_2\text{O})_2(\mathbf{L1})_6] \cdot 2\text{Br} \cdot \text{DMSO} \cdot 2(\text{H}_2\text{O})$ . The structure of complex **1** was determined by single crystal X-ray techniques with the structure solved in space group  $R\bar{3}$ . The crystals diffract as twins and were often weakly diffracting, however consistent unit cell parameters were obtained from several different sample batches. Samples were examined by either synchrotron or micro-source X-ray sources with the latter data preferred for refinement due to crystal decomposition in the brighter synchrotron beam. The asymmetric unit of the complex contains three crystallographically independent Cu(II) centers, three **L1** ligands, five coordinated  $\text{Br}^-$  ligands, one aquo ligand, three DMSO ligands, a solvent DMSO and disordered lattice  $\text{Br}^-$ . One methyl group and one pyridyl were modelled as disordered across two positions (Supplementary Information Fig.

1), although only a single position is shown in the Figures below. The coordination environments of each of the Cu(II) centers are similar, each with a square pyramidal geometry featuring an apical DMSO ligand, two trans iso-nicotinoyl groups from two **L1** ligands, and either two trans Br<sup>-</sup> anions or trans Br<sup>-</sup> and aquo ligands. The aquo ligand was distinguished through displacement parameters, and a substantially shorter Cu-O distance of 2.276(9) Å than was seen with Cu-Br separations which ranged between 2.447(4) and 2.528(6) Å.

Each **L1** ligand bridges between two Cu(II) centers through two of the three iso-nicotinoyl groups, leaving one iso-nicotinoyl group uncoordinated. These coordination interactions result in formation of [Cu<sub>6</sub>(**L1**)<sub>6</sub>] metallacycles where the uncoordinated iso-nicotinoyl groups and cavitated bowls of each **L1** are directed inwards (Fig. 2a). There are two distinct [Cu<sub>6</sub>(**L1**)<sub>6</sub>] rings within complex **1**, one of composition [Cu<sub>6</sub>Br<sub>6</sub>(DMSO)<sub>6</sub>(**L1**)<sub>6</sub>] and the other [Cu<sub>6</sub>Br<sub>4</sub>(DMSO)<sub>6</sub>(H<sub>2</sub>O)<sub>2</sub>(**L1**)<sub>6</sub>]<sup>2+</sup>, however the two rings are structurally very similar. The ligand enantiomer alternates around each [Cu<sub>6</sub>(**L1**)<sub>6</sub>] ring, meaning that each metallacycle is achiral. There are approximately 90° angles between two iso-nicotinoyl donor groups of an **L1** ligand and this ensures that the metallacycles are not planar, and have a chair-type conformation. Cu···Cu distances within each metallacycle are of the order of 19 Å for adjacent Cu centers and 37.5 Å across the ring. For both types of [Cu<sub>6</sub>(**L1**)<sub>6</sub>] rings, the terminal DMSO ligand bound to each Cu(II) centre is directed outwards from the metallacycle ring.

The metallacycles pack into 2D layers in the ab plane of the crystal lattice of **1** and finite groups of three adjacent metallacycles within these layers show a Borromean entanglement. Fig. 2b illustrates two adjacent [Cu<sub>6</sub>Br<sub>4</sub>(DMSO)<sub>6</sub>(H<sub>2</sub>O)<sub>2</sub>(**L1**)<sub>6</sub>]<sup>2+</sup> rings where there is an interdigitating overlap between the rings but no chain-link catenane formation. There are host-guest interactions between the two rings such that a coordinated DMSO ligand attached to one ring is directed into the molecular cavity of an **L1** host ligand of the other ring and vice versa. This association has a hydrophobic DMSO methyl group directed into the hydrophobic **L1** cavity. In Fig. 2c a third adjacent ring is included, this time of composition [Cu<sub>6</sub>Br<sub>6</sub>(DMSO)<sub>6</sub>(**L1**)<sub>6</sub>]. This metallacycle also forms host-guest associations with the two adjacent rings through the ligated DMSO guests and host **L1** ligands. These three metallacycles form a Borromean ring association where no two rings form a catenane, yet the three rings cannot be separated without breaking one of them. This can be most easily appreciated from the schematic of Fig. 2d where the metallacycles are shown with only the connectivity between the Cu(II) centres and **L1** ligands given. As can be seen, the grey ring loops under the green ring and over the purple ring; the green ring loops over grey and under purple, while the purple ring loops under grey and over green. This is equivalent to the Venn type Borromean rings shown in Fig. 1b(iii). These Borromean ring-type associations occur throughout

the 2D layer of metallacycles. Each metallacycle associates with six others in the *ab* plane and is party to six Borromean ring associations, Fig. 3a and in Supplementary Information Fig. 2. Each metallacycle in the 2D layer forms the same type of association with its neighbours; hence an infinite network of entangled macrocycles is created that resembles a chainmail, and the infinite pattern contains Borromean rings motifs, Fig. 3. The *trans*-(*iso*-nicotinoyl)<sub>2</sub>Cu(II) moieties of adjacent metallacycles within the chainmail roughly align (see Supplementary Information Fig. 3) with Cu···Cu separations of 4.39 or 4.40 Å and ring centroid separations between *iso*-nicotinoyl groups ranging from 4.15 to 4.29 Å. These distances are too long to indicate any substantial interaction.

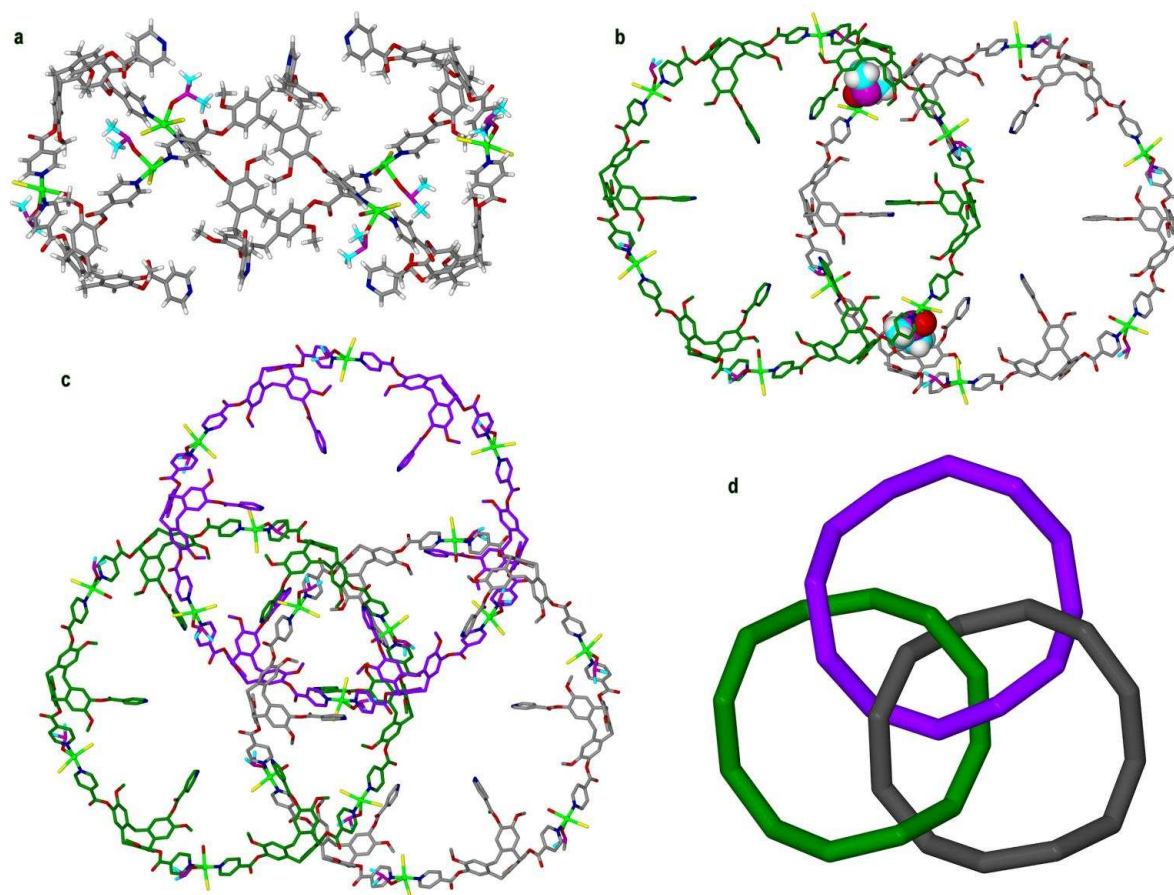


**Figure 2 Metallacycles and Borromean ring motifs from the crystal structure of complex 1. a,** Side-on view of a  $[\text{Cu}_6\text{Br}_4(\text{DMSO})_6(\text{H}_2\text{O})_2(\text{L}1)_6]^{2+}$  metallacycle. **b,** Two adjacent  $[\text{Cu}_6\text{Br}_4(\text{DMSO})_6(\text{H}_2\text{O})_2(\text{L}1)_6]^{2+}$  rings, the rings overlap but do not catenate and host-guest interactions between ligated DMSO of one ring and the **L1** cavity of another are highlighted with the DMSO guest in space-filling, consideration of three adjacent  $[\text{Cu}_6(\text{L}1)_6]$  rings (c) [two  $[\text{Cu}_6\text{Br}_4(\text{DMSO})_6(\text{H}_2\text{O})_2(\text{L}1)_6]^{2+}$  and one  $[\text{Cu}_6\text{Br}_6(\text{DMSO})_6(\text{L}1)_6]$  (in purple)] reveals a Borromean association with connectivity representation also shown in (d). Colour coding: pale green = Cu;

dark blue = N; red = O; yellow = Br; pink = S; white = H; grey/dark green/purple = C atoms of **L1**;  
light blue = C atoms of DMSO. Disordered groups shown in a single or averaged position.

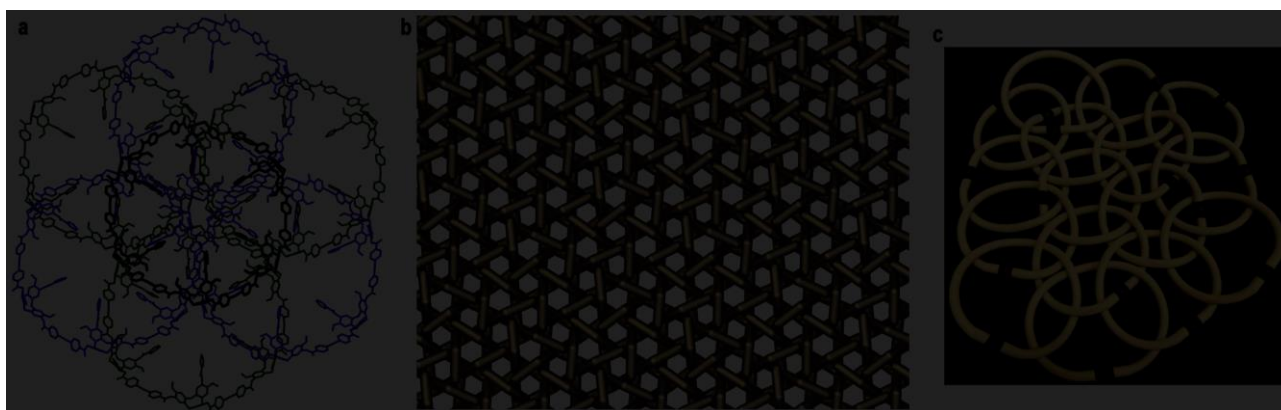


**Figure 3 Extended Borromean-ring motifs in complex 1.** **a**, One  $[\text{Cu}_6(\text{L1})_6]$  ring is shown forming six Borromean ring motifs with six other rings, the three rings of Fig. 2c are shown along with additional rings associating above (green) and below (purple) the central grey ring. **b**, Connectivity diagram of the 2D infinite chainmail motif. **c**, Construction model of the chainmail of complex.

Both Stoddart's and Jin's discrete Borromean rings are examples of orthogonal ring arrangements, Fig. 1b(i). In these ring-in-ring arrangements an interaction between an exo surface of one ring and an endo surface of the surrounding ring was either engineered through a templation strategy or was observed in the majority of examples. Stoddart's design used metal templation to bring together fragments of the macrocyclic rings in an endo and exo fashion,<sup>17</sup> and endo-exo weak ligand-metal interactions are observed between pairs of metallacycles in most examples of the Borromean metallacycles reported by Jin et al.<sup>18,19</sup> The Venn type Borromean arrangement of complex **1** also features endo-exo interactions between the rings through hydrophobic host-guest interactions between the molecular cavities of each **L1** ligand of a ring (the endo component) and the ligated DMSO of adjacent rings (the exo component). The chainmail of complex **1** is not Brunnian, meaning that the assembly cannot be pulled apart by cutting an individual link. Borromean rings are composed of three rings and are Brunnian. Hence the chainmail assembly of **1** is not itself a Borromean ring but rather is an infinite network that contains an infinite number of finite Borromean-ring associations. To the best of our knowledge, this represents a new and unclassified type of entanglement.

Not only is the entanglement of metallacycles in complex **1** new, it is, to the best of our knowledge, the first chemical example of a chainmail crystalline network involving macrocycles. A

chainmail requires chemically independent rings to be mechanically interlocked and can be characterized as a 0D (individual rings) to 2D (chainmail network) motif. Such a network has been envisaged through infinite [2]catenane links<sup>23</sup> but the closest examples have been [2]catenane infinite chains of metallacycles (0D to 1D),<sup>24,25</sup> and a 2D network where coordination chains of fused metallacycles link together through catenane formation (1D to 2D).<sup>26</sup> Polycatenation also occurs in organic polymers and oligomers.<sup>39,40</sup> Catenane chainmail motifs do occur in biology, notably in viral capsids.<sup>41</sup> There are also examples of coordination cages being linked through catenane formation into chain motifs,<sup>28</sup> and into 3D infinite frameworks.<sup>27</sup>

In the crystal lattice of **1** the metallacycle chainmail layers stack along the *c* crystallographic axis. Between the chainmail layers there are face-to-face  $\pi$ - $\pi$  stacking interactions between the uncoordinated iso-nicotinoyl groups of adjacent layers at ring centroid separations 3.67 and 3.78 Å, and between some phenyl groups at 3.64 Å, Fig. 4a. The manner in which the layers pack together creates small pockets within the lattice which are lined by the methylene groups of the **L1** ligands. There are two crystallographically distinct examples of these pockets, and they are occupied by Br<sup>-</sup> anions with C-H...Br distances ranging from 3.01 to 3.47 Å, consistent with the formation of multiple weak hydrogen bonds, Fig. 4b. Viewed down the *c* axis, the lattice shows channels of triangular cross-section which contain additional low occupancy Br<sup>-</sup> sites, and solvent DMSO (see Supplementary Information Fig. 4). Both microanalysis and thermal gravimetric analysis indicate that the level of solvation of the crystals is likely to be higher than was established through the crystal structure (see Supplementary Information), and void space exists within the lattice to accommodate additional solvent.

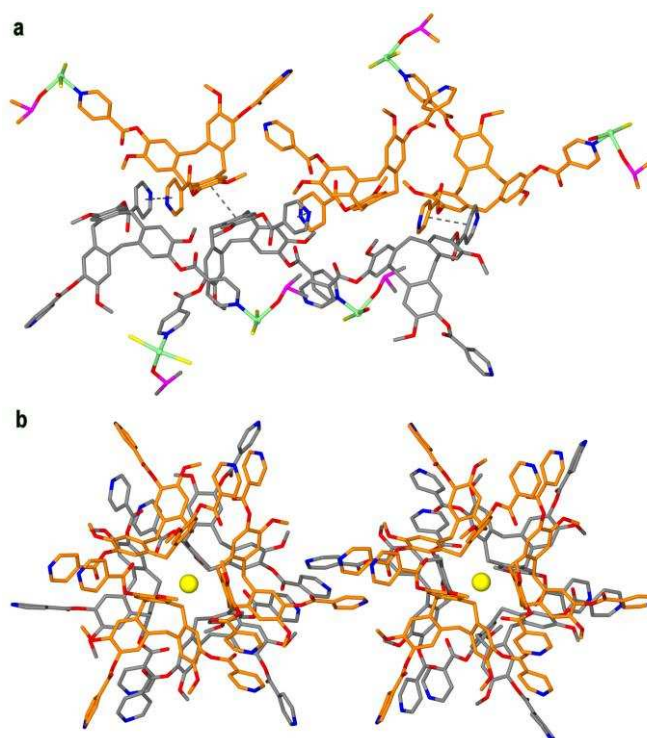


**Figure 4. Details from the crystal structure of complex 1 highlighting interactions between chainmail layers. a**,  $\pi$ - $\pi$  stacking interactions between layers shown with dashed lines. **b**,  $\text{Br}^-$  binding pockets within the crystal lattice with only **L1** ligands and  $\text{Br}^-$  (spheres) shown for clarity. The different layers are distinguished through different colours.

Bulk complex **1** can be re-dissolved (and indeed recrystallised) in hot DMSO solution, however DMSO is a coordinating solvent and this results in the break-up of the chainmail assembly and indeed breaks-up the  $[\text{Cu}_6(\text{L1})_6]$  metallacycles. Electrospray mass spectrometry (ES-MS) of the DMSO-digested complex only gave peaks corresponding to free ligand and smaller metal-ligand species such as  $\{\text{Cu}_4\text{Br}_5(\text{L1})_2\}^+$ ,  $\{\text{Cu}_3\text{Br}_3(\text{L1})_2\}^+$ ,  $\{\text{Cu}_2\text{Br}_2(\text{L1})\}^+$  and  $\{\text{CuBr}(\text{L1})_2\}^+$ , noting that some reduction of  $\text{Cu}^{\text{II}}$  to  $\text{Cu}^{\text{I}}$  has occurred during the ESI-MS experiment which is a known phenomenon.<sup>42</sup> Similarly, ES-MS of the reaction mixture taken prior to crystallisation did not show the presence of the metallacycles.

Crystals of complex **1** grow as clusters of hexagonal needles. The conditions for generating **1** are exacting. Use of different solvents, or common crystal growing strategies such as vapour diffusion of an anti-solvent, do not result in isolation of crystalline material, and reliable crystal growth occurs from the 2:1  $\text{Cu}(\text{II})\text{:L1}$  ratio despite the complex having 1:1 stoichiometry. Analogous complexes were not isolated through use of  $\text{CuCl}_2$  or  $\text{CuI}_2$  in place of  $\text{CuBr}_2$ . Powder X-ray diffraction indicates that the bulk material is predominantly one phase (see Supplementary Information) and that the material remains crystalline after drying under vacuum. Inspection by

optical microscopy and scanning electron microscopy (SEM) reveals that many of the crystals are hollow with an open-ended tube-like morphology. There was no bulk morphological differences observed between crystals kept under mother liquor and those dried under vacuum, and multiple batches of crystals gave similar morphologies. A selection of FEG-SEM images of different crystals of complex **1** is given in Fig. 5 and in Supplementary Information Figures 9-12. The holes that run through the crystals are aligned along the long needle axis and are macroscopic in size but do not occur uniformly throughout a batch. That is, the solid-shell-to-macropore ratio varies considerably from crystal to crystal. Fig. 5a for example, shows a crystal where there is only a thin shell of material surrounding the pore, while the crystal shown in Fig. 5b features a much thicker shell. Generally, the larger needles have thinner shells. Complex **1** was only observed to grow as clusters of needles from a solid central cluster core (Supplementary Information Fig. 11). Close inspection of the small solid needles reveals that some have a series of very small holes along the needle axis, Fig.5c. If the crystallising solutions are kept at low ambient temperatures (ca. 5-10 °C) and not initially heated then crystal growth is slowed down and nucleation does not occur until ca. two weeks have passed. These cold-crystallised crystals initially form as clusters of small solid needles with unit cell parameters consistent with complex **1**. If then left to stand in warmer conditions (ca. 15-20 °C) the small solid needles convert to clusters of much larger hollow tubular crystals. The initial solid needle-like morphology, Fig. 5d, can be trapped by recrystallisation at low concentrations (5 mg complex **1** in 3 mL DMSO). There were no major changes to morphologies observed for these after 4 weeks standing, including periods where the solution was kept at higher temperature. Keeping reaction solutions at higher temperatures (25 °C) gave no crystallisation over a period of many weeks, however crystals with the hollow tubular morphology were formed on cooling.

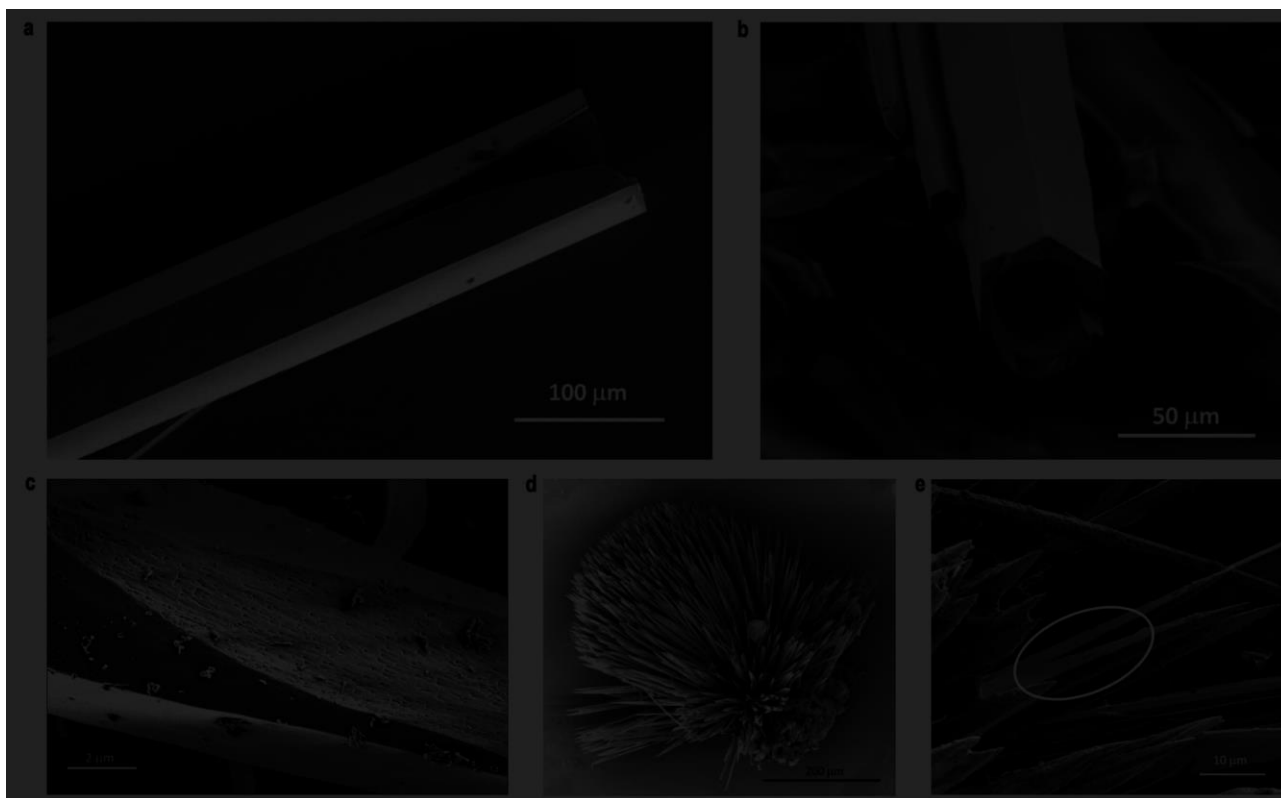


**Figure 5. FEG-SEM images of crystals of complex 1.** Images of the initially obtained crystals (**a** – **c**) where: **a**, example of a large tubular crystal; **b**, examples of tubular crystals and smaller rod-like crystals and needles; **c**, the end of a needle crystal with a series of small holes apparent. Images **(d)** and **(e)** are from a sample obtained from low concentration recrystallisation that results in mainly needle crystals being formed **(d)**, with circled section of **(e)** showing alignment of needles that may be a precursor to a tube (compare with **(a)**).

The formation of hollow, tubular crystals of organic material remains relatively rare but can occur through a number of proposed mechanisms. These include preferential dissolution of the centre of a rod-like crystal,<sup>43</sup> spontaneous dissolution-recrystallisation processes of single crystals<sup>44</sup> or of assemblies of precursor nanoparticles,<sup>45</sup> dissolution-recrystallisation processes induced by sonochemistry<sup>49</sup> or by solution-mediated dehydration or solvent-exchange of solvate crystals,<sup>46</sup> rolling up of layered crystals,<sup>47</sup> or through crystal growth under diffusion limited conditions with a high crystallisation rate.<sup>48</sup> The observations of complex **1** detailed above, notably the small holes in the small solid needles and formation of large tubular crystals from the solid needles on an increase in temperature (and thus solubility), are consistent with the tubular morphology being due to a spontaneous localised dissolution-recrystallisation process that occurs around the initial crystals. The manner in which the solid needles are aligned, see highlighted section of Fig. 5e, suggests that more than one needle may template the growth of each tubular crystal, which is consistent with the

twinned nature of the crystals. The behaviour of complex **1** in mother liquor is remarkably similar to the crystallisation behaviour reported by Su and co-workers for a Ag<sup>I</sup> coordination polymer with a Borromean weave entanglement.<sup>44</sup> They propose that their system initially grows as small rod-shaped crystals which undergo a rod-to-tube transformation through a localised dissolution-recrystallisation process.

In conclusion, the self-assembly and crystallisation of [Cu<sub>6</sub>Br<sub>n</sub>(**L1**)<sub>6</sub>] metallacycles has resulted in the formation of the first chemical example of a crystalline 0D to 2D infinite chainmail motif, and complements previously reported 0D to 1D<sup>24,25,28</sup> and 0D to 3D<sup>27</sup> crystalline assemblies. The chainmail does not form through catenane formation but rather features an infinite array of Borromean ring associations, again the first of its type. Use of a molecular host type ligand, such as the CTV-scaffold **L1**, may be a contributing factor to the formation of the chainmail as host-guest interactions form inter-ring endo-exo associations between metallacycles. Such interactions are relatively weak hence are not usually considered structure-directing, however as ES-MS studies show the metallacycles are not pre-formed in solution then they may have an important role here in bringing together the components in a structured fashion. Other types of topologically complex metallo-supramolecular assemblies with CTV-type ligands have been previously reported,<sup>10,11</sup> and it is notable that none of these assemblies were constructed using strong templating effects to achieve the threading or molecular entanglement. Leigh and co-workers have recently commented that “the control of molecular topology remains an almost entirely unconquered challenge for synthetic chemistry”<sup>3</sup> and serendipitous and previously unconsidered discoveries such as this one serve to further raise the challenge for ourselves and the synthetic supramolecular community at large.

## Methods

(±)-Tris(iso-nicotinoyl)cyclotriguaiacylene was synthesised according to literature methods,<sup>38</sup> and all other chemicals were obtained from commercial sources and were used as supplied.

**Synthesis of [Cu<sub>6</sub>Br<sub>10</sub>(DMSO)<sub>6</sub>(H<sub>2</sub>O)<sub>2</sub>(L1)<sub>6</sub>]·2Br·n(DMSO) (1)** (±)-Tris(iso-nicotinoyl)cyclotriguaiacylene (10 mg, 0.014 mmol) was dissolved in nitromethane (1 ml) and a CuBr<sub>2</sub> solution in DMSO (0.5 ml, 0.022 mol) was added. Further DMSO (0.4ml) was added to the solution and it was gently heated until dissolution was achieved. The brown solution was left to stand with crystals appearing after 3 days which were collected after two weeks of growth to give 5.6 mg of complex **1**. IR (ν cm<sup>-1</sup>) 1739 (CO<sub>2</sub>R), 1613 (C=C), 1505, 1447, 1417, 1325, 1264, 1205, 1175, 1139, 1100, 1059. Crystals were dried under vacuum prior to elemental analysis: observed C

50.00, H 4.00, N 3.90%, calculated for  $[\text{Cu}_6\text{Br}_{10}(\text{DMSO})_6(\text{H}_2\text{O})_2(\text{L1})_6]\cdot 2\text{Br}\cdot 3(\text{DMSO})\cdot 2(\text{H}_2\text{O})$  C 49.92, H 4.06 and N 3.91 %. ESI-MS (m/z)  $\{\text{Cu}^{\text{II}}\text{Br}(\text{L1})_2\}^+$  1590.2820, expected 1590.2909;  $\{(\text{Cu}^{\text{I}}\text{Br})(\text{Cu}^{\text{II}}\text{Br})(\text{L1})\}^+$  1734.1280, expected 1734.1375;  $\{(\text{Cu}^{\text{I}}\text{Br})_2(\text{Cu}^{\text{II}}\text{Br})(\text{L1})_2\}^+$  1877.9721, expected 1877.9839;  $\{(\text{L1})_2(\text{Cu}^{\text{II}}\text{Br}_2)_2(\text{Cu}^{\text{I}}\text{Br})(\text{Cu}^{\text{I}})\}^+$  2100.7372 expected 2100.7478. EDX analysis indicated the only heavy elements present are Cu, Br and S.

**X-ray structural analysis of 1.** A crystal of complex **1** was mounted on a MiTeGen loop under oil and X-ray diffraction data were collected on an Agilent SuperNova diffractometer with Cu-K $\alpha$  radiation ( $\lambda = 1.54184 \text{ \AA}$ ) at 100(1) K. Data were corrected for Lorentz and polarization effects and absorption corrections were applied using multi-scan methods. The structure was solved by direct methods and refined by block-matrix least-squares on  $F^2$  using the SHELX suit of programmes.<sup>50</sup> The crystals were twinned and the structure was refined using the twin law 0 1 0 1 0 0 0 -1. The batch scale factor refined to 0.551. All non-hydrogen atoms were refined anisotropically with restraints on displacement parameters, aside from some DMSO and partially occupied lattice Br-positions which were refined isotropically. One DMSO molecule was refined with bond length restraints and a group  $U_{\text{iso}}$ . Hydrogen atoms were included at calculated positions with a riding refinement. Crystal data for **1**:  $\text{C}_{266}\text{H}_{240}\text{Br}_{12}\text{Cu}_6\text{N}_{18}\text{O}_{63}\text{S}_7$ , Mr = 6261.34, trigonal (hexagonal axes),  $R\bar{3}$ , 0.20 x 0.02 x 0.02 mm, a = 38.1839(2), c = 57.9645(4)  $\text{\AA}$ , V = 73190(1)  $\text{\AA}^3$ , Z = 9,  $\rho_{\text{calc}} = 1.279 \text{ g cm}^{-3}$ , F(000) = 28548,  $\mu = 3.142 \text{ mm}^{-1}$ ,  $\theta_{\text{max}} = 51.27^\circ$ , 206597 reflections collected, 17582 unique ( $R_{\text{int}} = 0.0653$ ), 1603 parameters, 437 restraints,  $R_1 = 0.1302$  for 16158 reflections  $I > 2\sigma(I)$ ,  $wR_2 = 0.3698$  for all reflections, S = 1.796. CCDC-1030705 contains additional information in cif format and can be obtained from the CCDC via [www.ccdc.cam.ac.uk/data\\_request/cif](http://www.ccdc.cam.ac.uk/data_request/cif).

## Acknowledgements

We thank the EPSRC for funding this research, Tanya Marinko-Covell for microanalysis, Algy Kazlauciusas for EDX and TGA measurements and Dr Stuart Warriner for assistance with mass spectrometry. We thank Prof Stephen Hyde for useful discussion regarding topology. We acknowledge Diamond Light Source for time on beamline I19 under proposal MT8911.

## Author contributions

F. L. T.-G. and M. J. H. conceived and designed experiments. F. L. T.-G. performed synthetic, crystallographic and other characterisation experiments and A. N. K. performed SEM experiments. All authors contributed to analysis of the data. M. J. H. wrote the paper with discussions and contributions from F. L. T.-G. and some diagrams prepared by A. N. K.

## References

1. Sauvage, J.-P., Dietrich-Buchecker, C. O. (Eds.) *Molecular Catenanes, Rotaxanes and Knots. A journey through the world of molecular topology.* Wiley-VCH, Weinheim (1999).
2. Forgan, R. S., Sauvage, J.-P. & Stoddart, J. F. Chemical topology: complex molecular knots, links, and entanglements. *Chem. Rev.* **111**, 5434-5464 (2011).
3. Ayme, J.-F., Beves, J. E., Campbell, C. J. & Leigh, D. A. Template synthesis of molecular knots. *Chem. Soc. Rev.* **42**, 1700-1712 (2013).
4. Yang, W., Li, Y., Liu, H., Chi, L. & Li, Y. Design and assembly of rotaxane-based molecular switches and machines. *Small* **8**, 504-516 (2012).
5. Credi, A., Ventur, M. & Balzani, V. Light on molecular machines. *ChemPhysChem.* **11**, 3398-3403 (2010).
6. Ali, C., et al. High hopes: can molecular electronics realize its potential? *Chem. Soc. Rev.* **41**, 4827-4859 (2012).
7. Neal, E. A. & Goldup, S. M. Chemical consequences of mechanical bonding in catenanes and rotaxanes: isomerism, modification, catalysis and molecular machines for synthesis. *Chem. Commun.* **50**, 5128-5142 (2014).
8. Zhang, G., Presly, O., White, F., Oppel, I. M. & Mastalerz, M. A shape-persistent quadruply interlocked giant cage catenane with two distinct pores in the solid state. *Angew. Chem. Int. Ed.* **53**, 5126-5130 (2014).
9. Hasell, T., et al. Triply interlocked covalent organic cages. *Nature Chem.* **2**, 750-755 (2010).
10. Westcott, A., Fisher, J., Harding, L. P., Rizkallah, P. & Hardie, M. J. Self-assembly of a 3-D triply interlocked chiral [2]catenane. *J. Am. Chem. Soc.* **130**, 2950-2951 (2008).
11. Henkelis, J. J., Ronson, T. K., Harding, L. P. & Hardie, M. J.  $M_3L_2$  metallo-cryptophanes: [2]catenane and simple cages. *Chem. Commun.*, **47**, 6560-6562 (2011).
12. Wang, L., Vysotsky, M.O., Bogdan, A., Bolte, M. & Bohmer, V. Multiple catenanes derived from calix[4]arenes. *Science* **304**, 1312-1314 (2004).
13. Leigh, D. A., Pritchard, R. G. & Stephens, A. J. A Star of David catenane. *Nature Chem.* **6**, 978-982 (2014).

14. Niergarten, J.-F., Dietrich-Buchecker, C. O. & Sauvage, J.-P. Synthesis of a doubly interlocked [2]-catenane. *J. Am. Chem. Soc.* **116**, 375–376 (1994).
15. Mao, C., Sun, W. & Seeman, N. C. Assembly of Borromean rings from DNA. *Nature* **386**, 137-138 (1997).
16. Peters, A. J., Chichak, K. S., Cantrill, S. J. & Stoddart, J. F. Nanoscale Borromean links for real. *Chem. Commun.* 3394-3396 (2005).
17. Chichak, K. S., et al. Molecular Borromean rings. *Science* **304**, 1308-1312 (2004).
18. Huang, S.-L., Lin, Y.-J., Li, Z.-H. & Jin, G.-X. Self-assembly of molecular Borromean rings from bimetallic coordination rectangles. *Angew. Chem. Int. Ed.* **53**, 11218-11222 (2014).
19. Huang, S.-L., Lin, Y.-J., Hor, T. S. A. & Jin, G.-X. Cp\*Rh-based heterometallic metallarectangles: size-dependent Borromean link structures and catalytic acyl transfer. *J. Am. Chem. Soc.* **135**, 8125-8128 (2013).
20. Li, F., Clegg, J. K., Lindoy, L. F., Macquart, R. B. & Meehan, G. V. Metallosupramolecular self-assembly of a universal 3-ravel. *Nature Commun.* **2**, 205 (2011).
21. Carlucci, L., Ciani, G., Proserpio, D. M., Mitina, T. G. & Blatov, V. A. Entangled two-dimensional coordination networks: a general survey. *Chem. Rev.* **114**, 7557-7580 (2014).
22. Batten, S. R. Interpenetration, in *Supramolecular chemistry: from molecules to nanomaterials*, Gale, P. A. & Steed, J. W. (Eds) **6**, 3107-3120 (2012).
23. Carlucci, L., Ciani, G. & Proserpio, D. M. Polycatenation, polythreading and polyknotting in coordination network chemistry. *Coord. Chem. Rev.* **246**, 247-289 (2003).
24. Jin, C.-M., Lu, H., Wu, L.-Y & Huang, J. A new infinite inorganic infinite [n]catenane from silver and bis(2-methylimidazolyl)methane ligand. *Chem. Commun.* 5039-5041 (2006).
25. Loots, L. & Barbour, L. J. An infinite catenane self-assembled by  $\pi \cdots \pi$  interactions. *Chem. Commun.* **49**, 671-673 (2012).
26. Sagué, J. L. & Fromm, K. M. The first two-dimensional polycatenane: a new type of robust network obtained by Ag-connected one-dimensional polycatenes. *Cryst. Grow. Des.* **6**, 1566-1568 (2006).
27. Kuang, X., et al. Assembly of a metal-organic framework by sextuple intercatenation of discrete adamantane-like cages. *Nature Chem.* **2**, 461-465 (2010).

28. Heine, J., Schmedt auf der Günne, J. & Dehnen, S. Formation of a strandlike polycatenane of icosahedral cages for reversible one-dimensional encapsulation of guests. *J. Am. Chem. Soc.* **133**, 10018-10021 (2011).
29. Dolomanov, O. V., Blake, A. J., Champness, N. R., Schröder, M. & Wilson, C. A novel synthetic strategy for hexanuclear supramolecular architectures. *Chem. Commun.* 682-683 (2003).
30. Schmittel, M., et al. Cap for copper(I) ions! Metallosupramolecular solid and solution state structures on the basis of the dynamic tetrahedral  $[\text{Cu}(\text{phenAr}_2)(\text{py})_2]^+$  motif. *Inorg. Chem.* **48**, 8192-8200 (2009).
31. Loren, J. C., Yoshizawa, M., Haldimann, R. F., Linden, A. & Siegel, J. S. Synthetic approaches to a molecular Borromean link: two-ring threading with polypyridine templates. *Angew. Chem. Int. Ed.* **42**, 5702-5705 (2003).
32. Carlucci, L., Ciani, G. & Proserpio, D. M. Borromean links and other non-conventional links in 'polycatenated' coordination polymers: re-examination of some puzzling networks. *CrystEngComm* **5**, 269-279 (2003).
33. Pan, M. & Su, C.-Y. Coordination assembly of Borromean structures. *CrystEngComm* **16**, 7847-7859 (2014).
34. Hardie, M. J. Recent advances in the chemistry of cyclotrimeratrylene. *Chem. Soc. Rev.* **39**, 516-527 (2010).
35. Ronson, T. K., et al. Stellated polyhedral assembly of a topologically complicated  $\text{Pd}_4\text{L}_4$  'Solomon cube'. *Nature Chem.* **1**, 212-216 (2009).
36. Hardie, M. J. & Sumby, C. J. An interwoven 2-D coordination network prepared from the molecular host tris(isonicotinyl)cyclotriguaiacylene and silver(I) cobalt(III) bis(dicarbollide). *Inorg. Chem.* **43**, 6872-6874 (2004).
37. Ronson, T. K., Fisher, J., Harding, L. P. & Hardie, M. J. Star-burst prisms with cyclotrimeratrylene-type ligands: a  $[\text{Pd}_6\text{L}_8]^{12+}$  stella octangula. *Angew. Chem. Int. Ed.* **46**, 9086-9088 (2007).
38. Henkelis, J. J., et al. Metallo-cryptophanes decorated with bis-N-heterocyclic carbene ligands: self-assembly and guest uptake into a non-porous crystalline lattice. *J. Am. Chem. Soc.* **136**, 14393-14396 (2014).
39. Niu, Z. & Gibson, H. W. Polycatenanes. *Chem. Rev.* **109**, 6024-6046 (2009).

40. Fang, L., Olson, M. A., Benítez, D., Tkatchouk, E., Goddard, W. A. & Stoddart, J. F. Mechanically bonded macromolecules. *Chem. Soc. Rev.* **39**, 17-29 (2010).
41. Duda, R. L. Protein chainmail: catenated protein in viral capsids. *Cell* **94**, 55-60 (1998).
42. Hao, C. & March, R. E. Electrospray ionization tandem mass spectrometric study of salt cluster ions: Part 2 – Salts of polyatomic acid groups and of multivalent metals. *J. Mass. Spectrom.* **36**, 509-521 (2001).
43. Zhao, Y. S., et al. Optical waveguide based on crystalline organic microtubes and microrods. *Angew. Chem. Int. Ed.* **47**, 7301-7305 (2008).
44. Zhang, X.-L., et al. Discrete chiral single-crystal microtubes assembled with honeycomb coordination networks showing structural diversity and Borromean topology in one single crystal. *Chem. Mater.* **19**, 4630-4632 (2007).
45. Ma, Y., Börner, H. G., Hartmann, J. & Cölfen, H. Synthesis of DL-Alanine hollow tubes and core-shell mesostructures. *Chem. Eur. J.* **12**, 7882-7888 (2006).
46. Ulrich, J., Schuster, A. & Stelzer, T. Crystalline coats or hollow crystals as tools for product design in pharmaceutical industry. *J. Cryst. Growth* **362**, 235-237 (2013).
47. Chen, Y., Zhu, B., Zhang, F., Han, Y. & Bo, Z. Hierarchical supramolecular self-assembly of nanotubes and layered sheets. *Angew. Chem. Int. Ed.* **47**, 6015-6018 (2008).
48. Eddleston, M. D. & Jones, W. Formation of tubular crystals of pharmaceutical compounds. *Cryst. Grow. Des.* **10**, 365-370 (2010).
49. Sander, J. R. G., Bučar, D.-K., Baltrusaitis, J. & MacGillivray, L. R. Organic nanocrystals of the resorcinarene hexamer via sonochemistry: evidence of reversed crystal growth involving hollow morphologies. *J. Am. Chem. Soc.* **134**, 6900-6902 (2012).
50. Sheldrick, G. M. A short history of SHELX. *Acta Cryst.* **A64**, 112-122 (2008).

## Table of contents summary

[Cu<sub>6</sub>L<sub>6</sub>] metallacycles where L = tris(iso-nicotinoyl)cyclotriguaiacylene have a unique topological entanglement in the solid state. Individual metallacycles are interwoven into an infinite 2D chainmail network where each metallacycle forms multiple Borromean ring-like associations with its neighbours. Crystals of the complex grow in an unusual tubular morphology.

